

THE INVESTIGATION OF THE PORE STRUCTURE OF FINE ALUMINA POWDERS PREPARED FOR CERAMIC PRODUCTION BY THE TECHNIQUE OF PRECIPITATION FROM SOLUTION

K. ADA ¹, Y. SARIKAYA ², T. ALEMDAROĞLU ² and M. ÖNAL ²

¹ *Kırıkkale University, Faculty of Science and Literature, Department of Chemistry, Kırıkkale, Turkey*

² *Ankara University, Faculty of Science, Department of Chemistry, Tandoğan, 06100 Ankara, Turkey*

(Received Oct. 11, 2000; Accepted Nov. 15, 2000)

ABSTRACT

In this study, alumina precursors were prepared in three different ways and were converted into three different alumina powders (Al_2O_3) by calcination. The precipitation methods of the alumina precursors were as follows: i) Addition in excess of a 25% NH_3 solution dropwise for two hours, to a boiling 0.08 M $\text{Al}_2(\text{SO}_4)_3$ solution which was already buffered by $\text{NH}_3 / \text{NH}_4\text{Cl}$. ii) Boiling for two hours a 0.006 M $\text{Al}_2(\text{SO}_4)_3$ solution which contains $\text{C}_2\text{H}_4(\text{COOH})_2$, NH_4Cl and $(\text{NH}_2)_2\text{CO}$. iii) Boiling for two hours a 0.2 M $\text{Al}_2(\text{SO}_4)_3$ solution which contains excess $(\text{NH}_2)_2\text{CO}$. In order to find out the effect of the followed procedure on the pore structure, the following determinations were realized. The powder shapes and sizes were determined by electron microscopy. The specific surface areas and the adsorption heats of these powders were calculated from the adsorption data. The mesopore size distribution curves were plotted by using the desorption data. The specific micropore, mesopore and micropore-mesopore volumes were determined by extrapolating these curves. Finally, the dependence of the pore structure on the procedure of preparation was discussed in detail.

INTRODUCTION

The most used material in high technology ceramics is alumina ^{1,2}. The first and most important step in the production of alumina is the preparation of fine alumina powders ^{3,4}. In order to provide closest spherical packing during the forming, the powder particles should be in the form of smallest possible, equally sized and inagglomerated spheres ^{5,6}.

The empty spaces in and between the particles are called pores. These pores are assumed to be cylindrical. A pore whose radius is smaller than 1nm is called a micropore, whose radius is between 1nm and 25 nm is called a mesopore and whose radius is bigger than 25 nm is called a macropore ⁷. The porosity of ceramics depends largely on the porosity of the powders. The porosity affects the mechanical,

thermal, electrical, transparency and optical properties of ceramics. Therefore, the aluminas, which will be used as structural materials are produced as nonporous, whereas the aluminas, which will be used as catalyst beds and filters are produced to have porosity to a certain extent^{8,9}.

The porosity of fine alumina powders changes depending on the procedures and conditions of preparation. The aim of this study was the investigation of the pore structures of fine alumina powders, which were prepared according to three different procedures.

EXPERIMENTAL PROCEDURE

Analytically pure $\text{Al}_2(\text{SO}_4)_3 \cdot 18 \text{H}_2\text{O}$, $(\text{NH}_2)_2\text{CO}$, $\text{C}_2\text{H}_4(\text{COOH})_2$, NH_4Cl , 65 % HNO_3 whose density is 1.40 g cm^{-3} and 25 % NH_3 solution whose density is 0.91 g cm^{-3} were supplied by Merck. A stock solution of 0.4 M $\text{Al}_2(\text{SO}_4)_3$ was prepared by adding a small amount of nitric acid.

In the first preparation procedure, $\text{Al}_2(\text{SO}_4)_3$ solution (200 cm^3 ; 0.08M), which was prepared from the stock solution was buffered by $\text{NH}_3 / \text{NH}_4\text{Cl}$. The first $\text{Al}(\text{OH})_3$ was precipitated by adding the ammonia (25 % NH_3) solution dropwise to the boiling solution for 2 hours. This precursor was filtered while it was hot and washed with distilled water until it did not contain any Cl^- , NO_3^- , and SO_4^{2-} ions. Afterwards, it was dried for 2 hours at 100°C . The dried precursor was calcined for 2 hours at 1000°C and the first fine alumina (Al_2O_3) powder which was labeled as P1 was obtained.

In the second preparation procedure, NH_4Cl (10 g), $(\text{NH}_2)_2\text{CO}$ (4 g) and $\text{Al}_2(\text{SO}_4)_3$ (2.5 cm^3 from 0.4 M stock solution) was added to $\text{C}_2\text{H}_4(\text{COOH})_2$ (5 g) solution in water (100 cm^3). Then, it was diluted to 400 cm^3 by distilled water. This solution in which the Al^{3+} concentration was 0.006 M was boiled for 2 hours. During the boiling process, NH_3 was produced as a result of the thermal decomposition of $(\text{NH}_2)_2\text{CO}$. Hence the solution was buffered by $\text{NH}_3 / \text{C}_2\text{H}_4(\text{COONH}_4)$. Thus, the second $\text{Al}(\text{OH})_3$ was precipitated. The same procedure to get the first precipitate was applied to this precipitate and the second fine alumina powder, which was later labeled as P2 was obtained.

In the third preparation procedure, the NH_3 that will precipitate Al^{3+} ions is formed in the solution by the thermal decomposition of $(\text{NH}_2)_2\text{CO}$. It was experimentally determined that, in order supply the necessary amount of NH_3 that will precipitate the

Al^{3+} ions, the amount of excess $(\text{NH}_2)_2\text{CO}$ in the solution has to satisfy the condition of $(\text{NH}_2)_2\text{CO} / (\text{Al}^{3+}) = 10.8$. According to this condition, $(\text{NH}_2)_2\text{CO}$ (2.6 g) was dissolved in the stock $\text{Al}_2(\text{SO}_4)_3$ solution (200 cm^3) and the solution was diluted to 800 cm^3 by distilled water. The concentration of the Al^{3+} ions in the solution is 0.2 M. By using the solubility product (1.9×10^{-33}) of $\text{Al}(\text{OH})_3$ and the ionization product of water (10^{-14}), the pH value that is necessary to precipitate 0.2M Al^{3+} ions was calculated as 3.34. The pH of the solution was increased to this value by adding NH_3 solution, dropwise. This solution was boiled by stirring with a

magnetic stirrer, for two hours. The third $\text{Al}(\text{OH})_3$ was precipitated by bubbling NH_3 , which was formed by the thermal decomposition of $(\text{NH}_2)_2\text{CO}$ during the boiling process. Afterwards the same procedure to get the first precipitate was applied to this precipitate and the third fine alumina powder, which was labeled as P3 was obtained.

The P1, P2 and P3 powders, whose precursors were obtained via different procedures, were investigated by an electron microscope (JEOL, JSM U-3). The adsorption and desorption of nitrogen on the same powders was realized at the temperature of liquid nitrogen ($T \approx 77\text{K}$), by the help of a volumetric adsorption instrument which is fully constructed of pyrex glass and connected to high vacuum

RESULTS AND DISCUSSION

Electron Microscopy

The photographs, taken by an electron microscope, of the particles in the fine alumina powders P1, P2 and P3 are, respectively, shown in Figures 1-3. It can be clearly observed from these figures that the shapes and sizes of the alumina particles depend on the procedure followed for the preparation of the precursors. The precipitation of $\text{Al}(\text{OH})_3$, by ammonia, from the Al^{3+} solution, which was buffered by $\text{NH}_3 / \text{NH}_4\text{Cl}$, is known as the conventional method. It is clearly observed in the photograph given in Fig. 1. that the Al_2O_3 powders are shapeless. These kinds of particles can not form hexagonal closest packing during the shaping process. Therefore, it is impossible to produce alumina materials of high mechanical strength by the powders formed of these kinds of particles, however, they can be used in the production of catalyst beds and diaphragms, where the mechanical strength does not carry great importance.

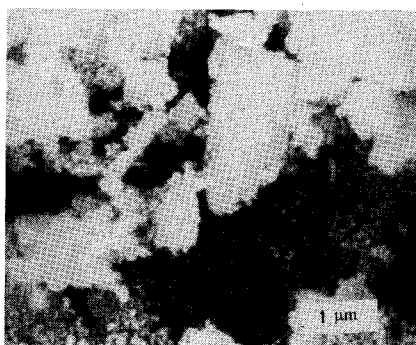


Figure 1. The electron microscopy photograph of the Al_2O_3 powder (P1) which was obtained by the calcination of $\text{Al}(\text{OH})_3$ precursor at 1000°C , which in turn was precipitated by excess NH_3 from the 0.08M Al^{3+} solution which was buffered by $\text{NH}_3 / \text{NH}_4\text{Cl}$.

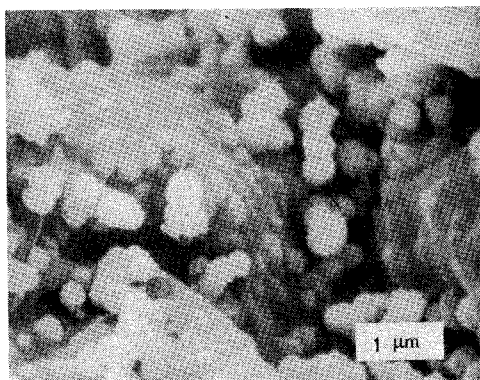


Figure 2. The electron microscopy photograph of the Al_2O_3 powder (P2) which was obtained by the calcination of $\text{Al}(\text{OH})_3$ precursor at 1000°C , which in turn was precipitated by bubbling NH_3 , which was formed by the thermal decomposition of excess $(\text{NH}_2)_2\text{CO}$, from the 0.06M Al^{3+} solution which was buffered by $\text{NH}_3 / \text{C}_2\text{H}_4(\text{COONH}_4)_2$.

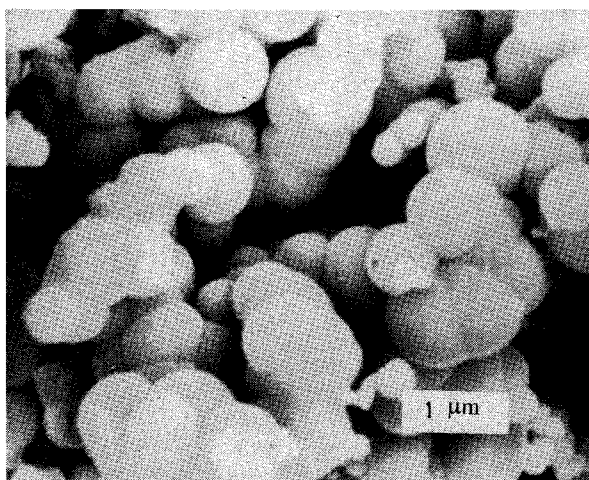


Figure 3. The electron microscopy photograph of the Al_2O_3 powder (P3) which was obtained by the calcination of $\text{Al}(\text{OH})_3$ precursor at 1000°C , which in turn was precipitated by bubbling NH_3 , which was formed by the thermal decomposition of $(\text{NH}_2)_2\text{CO}$, from the 0.2M Al^{3+} solution.

The P2 powder was obtained from the precursor which was precipitated by the thermal decomposition of $(\text{NH}_2)_2\text{CO}$, from the Al^{+3} solution which was buffered by

$\text{NH}_3 / \text{C}_2\text{H}_4(\text{COONH}_4)_2$. It is observed from the photograph seen in Fig.2 that, in the P2 powder, besides the shapeless particles there are also spherical particles which are not equally sized. The difference, which occurs in the shapes and sizes of the particles, when the starting mixture changes, shows that the path followed for the preparation of the precursor is very important.

The precipitation of $\text{Al}(\text{OH})_3$ from the Al^{3+} solution, by the bubbling NH_3 which is formed by the thermal decomposition of $(\text{NH}_2)_2\text{CO}$, is known as an unconventional method. It is clearly seen in the photograph of Fig. 3 that, the powder P3, which was prepared from the precursor, which was prepared by this method, consists mainly of agglomerated spherical particles. The formation of agglomerated particles, which prevents closest spherical packing during the forming process, is an unwanted event. The average size of independent particles and the average size of agglomerated particles were, determined, respectively, as $5\mu\text{m}$ and $60\mu\text{m}$, by using a large number of photographs, taken by electron microscope. It was determined that, the heating rate, the concentration of the Al^{3+} and the (urea) / (Al^{3+}) ratio had an effect on the size and agglomeration of the particles.

Adsorption of Nitrogen

It was not possible to obtain information about the porosity inside the particles, from the photographs taken by electron microscope. The micro- and mesopore structures of the particles were investigated by using the data of adsorption and desorption of nitrogen at 77K. The isotherms of the adsorption and desorption of nitrogen at 77K, on the powder P1 are given in Fig. 4. In this figure; p is the equilibrium pressure of the adsorption or desorption, p^0 is the saturated vapor pressure of liquid nitrogen at the temperature of the experiment, p/p^0 is the relative equilibrium pressure of the adsorption or desorption and n is the adsorption capacity, which is defined as the amount of nitrogen that is bound on one gram of powder. The rapid increase in the adsorption isotherm of the powder, P1, as the pressure, p/p^0 , approaches zero shows that a small number of micropores exist in the Al_2O_3 particles. By using the data of adsorption, a graph can be plotted according to the following Brunauer, Emmett and Teller (BET) equation^{7,11}

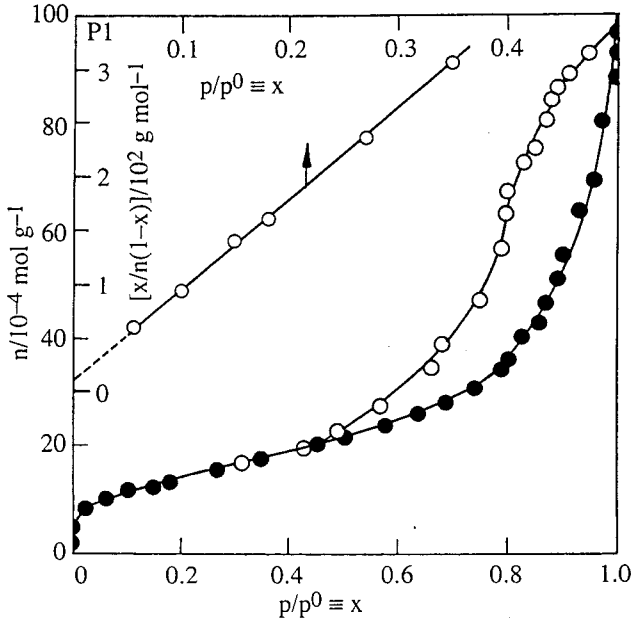


Figure 4. The adsorption isotherm (\square), desorption isotherm (\circ) and BET straight line obtained by the adsorption and desorption of nitrogen on the powder, P1, at 77 K.

$$x / [n(1-x)] = 1 / (n_m c) + [(c-1) / (n_m c)] x \quad (1)$$

where, n_m is the monomolecular adsorption capacity, c is a constant which is related to the heat of adsorption. The fact that this graph gives a straight line in the interval between $0.05 < x < 0.35$, shows that the adsorption is multimolecular (Fig.4). The n_m and c values, which were calculated simultaneously from the equations which were obtained from the slope and the intercept of the BET straight line on the vertical axis, are given in Table 1. The specific surface area (A)^{7,12}, which is defined to be equal to the area of the walls of the pores in one gram of the solid was calculated from the following relationship and given in Table 1⁷.

$$A = n_m N_A a_M \quad (2)$$

Here, $N_A = 6.02 \times 10^{23} \text{ mol}^{-1}$ is the Avogadro constant and $a_M = 16.2 \times 10^{-20} \text{ m}^2$ shows the area that one nitrogen molecule covers. On the other hand, the heat of adsorption (q) was calculated from the following relationship and given in Table 1.

$$q = q_1 - q_L = RT \ln c \quad (3)$$

Here, q_1 is the heat of adsorption of the first layer, $q_L = 5577 \text{ J mol}^{-1}$ is the heat of condensation of nitrogen, R is the universal gas constant and T is the temperature of adsorption. It can be observed from Fig. 4 that there is a rather large hysteresis between the isotherms of the adsorption and desorption of the powder P1. It was thought that this situation was related to the noncylindrical forms of the pores. The shape of the desorption isotherm, in the relative equilibrium pressure interval between $0.96 < x < 0.35$ shows the capillary evaporation of nitrogen which was bound on the particles. This attitude means that the particles are rather mesoporous.

The radii of the pores, which were assumed to be cylindrical were calculated from the following corrected Kelvin equation⁷, by using the data of desorption.

$$r / \text{nm} = 0.952 / \ln x + 0.735 / (\ln x)^{1/3} \quad (4)$$

The specific micro- and mesopore volumes of the pores, which have radii equal to the value calculated from the above relationship or radii which are smaller than the calculated value were calculated from the following relationship. It was assumed that they were equal to the volume of liquid nitrogen inside these pores.

$$v^l = n V^l \quad (5)$$

where, $V^l = 34.65 \text{ cm}^3 \text{ mol}^{-1}$ is the molar volume of liquid nitrogen, n is the adsorption capacity which is taken from the data of desorption as the relative equilibrium pressure decreases in the interval between $0.96 < x < 0.35$. The $v^l - r$ mesopore size distribution curve of the powder P1 is presented in Fig. 5. The specific micropore volume (v_{mi}^l) and the specific micropore-mesopore volume (v_{mm}^l) were, respectively, found from the extensions of the $v^l - r$ curve to, respectively, $r = 1 \text{ nm}$ and $r = 25 \text{ nm}$ and given in Table 1. The specific mesopore volume was calculated from the following relationship and given in Table 1.

$$v_{me}^l = v_{mm}^l - v_{mi}^l \quad (6)$$

It can be observed from Fig. 6 that the adsorption and desorption isotherms coincide. This coincidence shows that the mesopores are cylindrical. By inspecting the shapes of the adsorption and desorption isotherms, it can be stated that the particles of the powder P2 do not contain any micropores, they contain a small amount of mesopores and they contain a large amount of macropores. The BET straight line of this powder is also seen in Fig. 6. The values n_m , c , A and q which were calculated simultaneously from the slope and the intercept on the vertical axis of this straight line are given in Table 1. The $v^l - r$ mesopore size distribution curve of the powder, P2, is given in Fig. 7. The specific volumes, v_{mm}^l , v_{mi}^l and v_{me}^l , which were calculated as defined above are given in Table 1. The adsorption and desorption isotherms and the BET straight line of the powder, P3, are given in Fig. 8. The hysteresis between the adsorption and desorption isotherms is rather small showing

that the mesopores in this powder have an almost cylindrical shape. The values, n_m , c , A and q which were calculated from the BET straight line of the powder, P3, are given in Table 1. The $v^I - r$ mesopore size distribution curve of this powder is seen in Fig. 9. The values, v_{mm}^I , v_{mi}^I and v_{me}^I , which were calculated as defined above are given in Table 1.

Table 1. Some parameters related to the porosity of fine alumina powders which were prepared via different procedures.

Sample	$\frac{n_m}{10^{-3} \text{ mol g}^{-1}}$	$\frac{A}{\text{m}^2 \text{ g}^{-1}}$	$\frac{C}{\text{unitless}}$	$\frac{q}{\text{kJ mol}^{-1}}$	$\frac{q_l}{\text{kJ mol}^{-1}}$	$\frac{v_{mm}^I}{\text{cm}^3 \text{ g}^{-1}}$	$\frac{v_{mi}^I}{\text{cm}^3 \text{ g}^{-1}}$	$\frac{v_{me}^I}{\text{cm}^3 \text{ g}^{-1}}$
P1	1.18	115	84.6	2841	8420	0.33	0.04	0.29
P2	0.75	73	1.48	251	5830	0.60	0.00	0.60
P3	0.72	70	69.6	2714	8290	0.14	0.04	0.10

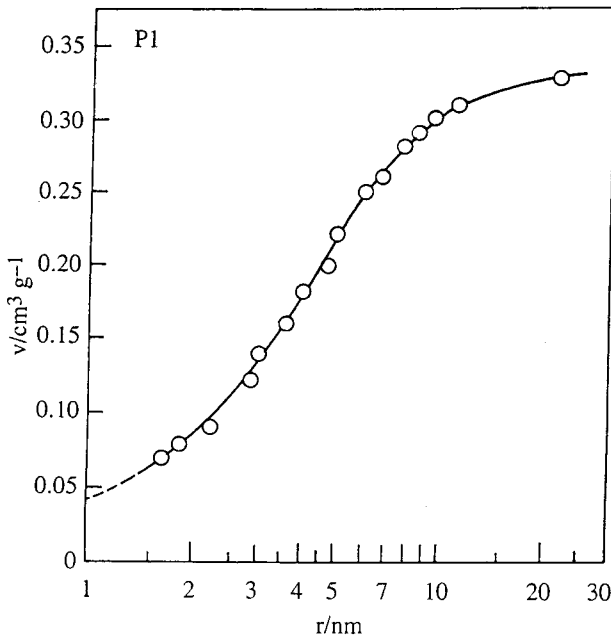


Figure 5. The curves of mesopore size distribution in the particles which form the powder, P1.

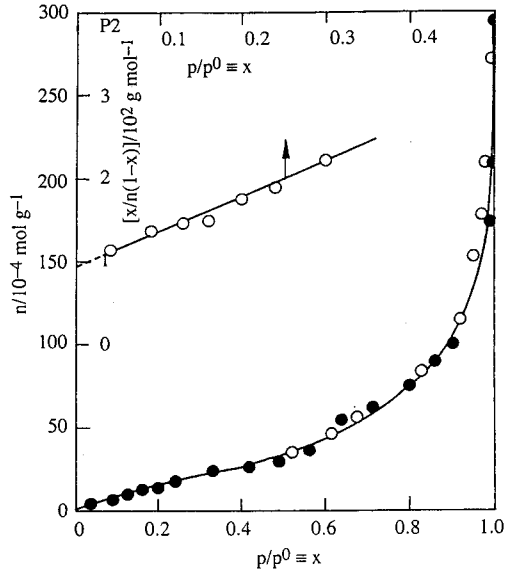


Figure 6. The adsorption isotherm (\square), desorption isotherm (\circ) and BET straight line obtained by the adsorption and desorption of nitrogen on the powder, P2, at 77 K.

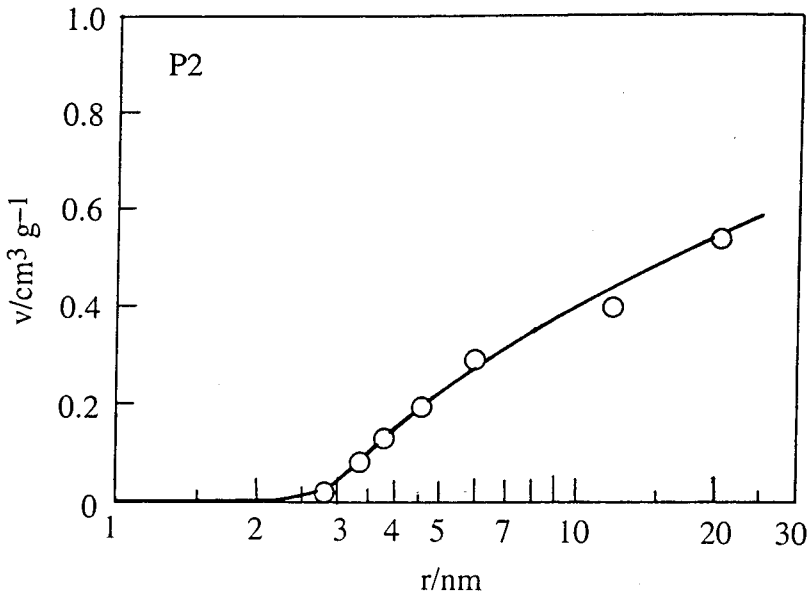


Figure 7. The curves of mesopore size distribution in the particles which form the powder, P2.

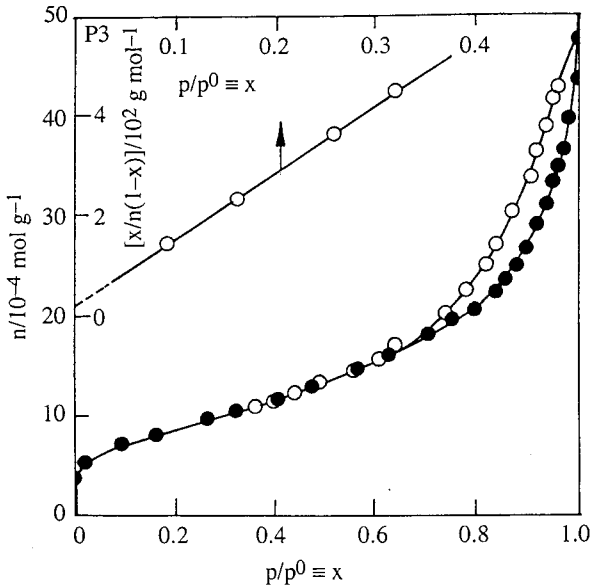


Figure 8. The adsorption isotherm (\square), desorption isotherm (\circ) and BET straight line obtained by the adsorption and desorption of nitrogen on the powder, P3, at 77 K.

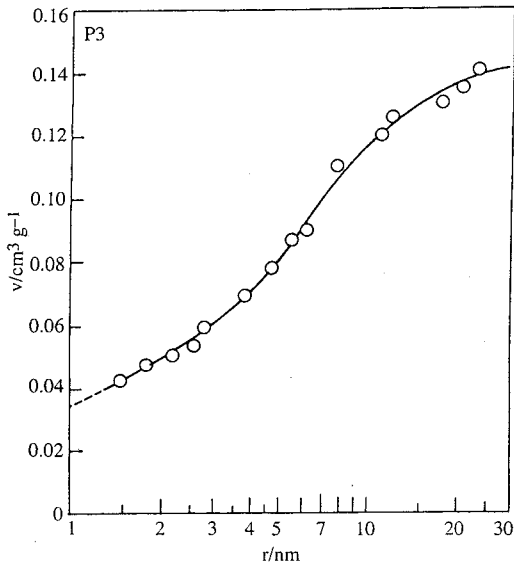


Figure 9. The curves of mesopore size distribution in the particles which form the powder, P3.

CONCLUSION

It was observed that the pore structure of the fine alumina powders varied considerably depending on the preparation procedures of the precursors. The A and q values of the particles of the powder, P1, are greater than the others. This fact shows that these particles consist of a small number of micropores whose surfaces are considerably active and a large number of mesopores of small radii. Although the A value of the powder, P2, was not very small the q value was small. The explanation of this attitude may be that these particles did not contain any micropores but they contained mesopores of large radii whose surface activities were rather low. The fact that the specific mesopore volume of the powder, P2, was the largest supports this idea. It was determined that although the A and q values of the powder, P3, were not very small the v_{mes} value was rather low. This attitude was related to the fact that these particles contained micropores as well as mesopores of small radii.

ACKNOWLEDGMENT

The authors thank the Ankara University Research Fund for funding this work by the project 96-25-00-18.

REFERENCES

- [1] Gitzen, H. W. *Alumina as a Ceramic Material*, The American Ceramic Society Publication: Ohio, 1970.
- [2] Dorre, E.; Hübner, H.; Ilschner, B.; Grand, N. J. *Alumina: Processing, Properties and Applications*, Springer Verlag, Berlin, 1984.
- [3] Johnson Jr. D. W. *Am. Ceram. Soc. Bull.* 1981, 60, 221.
- [4] Richardson, K.; Akınç, M. *Ceram. Inter.* 1988, 13, 253.
- [5] Sordalet, D.; Akınç, M. *J. Coll. Inter. Sci.* 1988, 122, 47.
- [6] Sarıkaya, Y.; Akınç, M. *Ceram. Inter.* 1988, 14, 239.
- [7] Gregg S. J.; Sing, K. S. W. *Adsorption, Surface Area and Porosity*, 2nd ed., Academic Press, London, 1982.
- [8] Hugo, P.; Koch, H. *Ger. Chem. Eng.* 1979, 2, 24.
- [9] Sevinç, İ.; Sarıkaya, Y.; Akınç, M. *Ceram. Inter.* 1991, 17, 1.
- [10] Sarıkaya, Y.; Aybar, S. *Commun. Fac. Sci. Uni. Ank.* 1978, 24, 33.
- [11] Brunauer, S.; Emmett, P. H.; Teller, E. *J. Am. Chem. Soc.* 1938, 60, 309.
- [12] Ceylan, H.; Sarıkaya, Y. *Doğa, TU Kim. D. C.* 1988, 12, 147.